Simplified Transfer Function Approach of Rubber Bushing Damping Characteristics for Accurate Prediction of Durability Loads in Multi-Body Dynamics Models

ABSTRACT

Physical systems that consist of parts and vibration isolators such as bushings or mounts are usually modelled in multi-body simulations where parts are represented as rigid bodies using their mass and inertia properties and Voigt models are used for isolators to represent dynamic characteristic of the physical system as accurately as possible. Employment of Voigt models in multi-degree-of-freedom (MDOF) systems, however, may result in low accuracy models due to limitations in representing frequency-dependent dynamic characteristics and its modelling complexity. To overcome this challenge, in this study, we develop and present a simplified frequency-dependent transfer function model, which allows for a more accurate determination of the bushing forces by generating frequency dependent complex stiffness and damping characteristics of the rubber bushings from vehicle level measurements. The proposed methodology is demonstrated on a MDOF heavy commercial vehicle cabin system to simplify the model and represent its dynamic characteristic with transfer function model instead of Voigt model. Simulation results are well correlated with the measurements obtained from prototype vehicle measurements on various durability roads over the frequency range of interest showing capability improvement over Voigt modeling approach. Integration of the proposed method into multi-body simulation software is also demonstrated with co-simulation between MSC.ADAMS and MATLAB software.

Keywords: Multibody dynamics, rubber bushings, frequency-dependent stiffness, damping, cabin suspension design, simplified transfer function model

1. INTRODUCTION

Development of a vehicle has become more challenging due to ever increasing competition and more efficient product demands from

customers. Therefore, use of analytical design processes has become an essential part of the vehicle product development cycle. More specifically, efficient analytical tools must replicate the real life scenarios more accurately. This in turn will enable the design of a product with less physical testing in a much shorter time.

Analytical calculation of the vehicle performance in early phases of vehicle development process enables assessment of new designs in terms of durability, driving dynamics, noise and vibration performance without requiring many physical prototypes in the product development cycle. To address these needs, versatile and efficient, state of the art simulation methods are needed that allow for the successful prediction of dynamic systems' responses under real life conditions. This in turn is a very challenging task for a variety of reasons. Customer's expectations from a vehicle design has increased significantly on many attributes such as durability, vehicle dynamics, performance and fuel economy. Needless to say, these attributes are usually in conflict. Durability of a vehicle in general requires heavier body components with high strength properties to be used whereas vehicle performance, fuel economy and emissions call for lighter vehicles. To design the vehicles as light as possible and optimize the trade-offs between various attributes, the engineers should be able to calculate the loads acting on the vehicle accurately under real life condition. A key challenge for calculating the loads depends on the quality of the simulation model where the quality refers to both the accuracy of the simulation outputs and its complexity in terms of model inputs. A useful simulation model should be as accurate as possible with the least amount of complexity in order to replicate the real life conditions.

It is not uncommon to build and use a very complex model of the system during the vehicle development cycle. This should reduce costs and development time. However, the determination of the model parameters can require more hardware and measurement time, which may add significantly to the cost. Therefore, it is desirable to create computer simulation models with minimum complexity. Another disadvantage of the simulation models is related to their computational time requirement, especially when the models are to be evaluated multiple times in design optimization studies (Papalambros and Wilde, 2000). For example, typical automotive models are comprised of more than 250 rigid bodies, and more than 1100 degrees of freedom, which result in long simulation times (Tuncel et. al., 2010).

Another challenge in addition to the complexity of the simulation model is the determination of simulation parameters. More specifically, the inputs of a generic multibody dynamics based simulation model include the

mass, inertia, center of mass of the rigid bodies as well as the viscoelastic properties of the joints between the rigid bodies. The parameters for mass, inertia and center of mass of the rigid bodies are usually straightforward to obtain. However, viscoelastic properties of the joints are usually difficult to obtain and their implementation in the simulation software is more complicated. The viscoelastic properties, which play an important role in ride comfort and loads acting at the attachment points where these elements are used, are in general highly nonlinear. Their stiffness and damping properties are dependent on both frequency and amplitude of excitation (Sedlaczek et. al., 2011). In literature, Voigt model (Zhang et. al., 2011 and Cao et. al., 2005) is the most commonly used analytical model to represent the viscoelastic properties of rubber bushings in the dynamic simulation of vehicles. However, quasi-static force-deflection tests suggest that bushings can be characterized as a non-linear stiffness with energy dissipation due to viscous damping and material friction, which cannot be modelled with the use of Voigt parameters only. The dynamic sweep tests of the bushings show that stiffness and phase angle both slightly increase over frequency while their damping exponentially decreases due to high viscous damping at lower frequencies (Scheiblegger, et. al., 2014). Despite the frequent usage of Voigt models in multi-body simulations, they are limited to predict the dynamic behavior of the vehicle response accurately for the whole frequency range of interest but only capable of predicting the system dynamics when the frequency of interest corresponds to a single one (Lee and Kim, 2002), which is around the resonant frequency of a Single Degree-of-Freedom (SDOF) system (Scheiblegger, et. al., 2014).

Many different viscoelastic vibration isolator models have been proposed (Li et. al., 2015, Scheiblegger et. al., 2014, Lee and Kim, 2002) to improve the Voigt model for its known deficiencies. For example, Li et. al., (2015) and Scheiblegger et. al. (2014) proposed a bushing model, which includes hysteresis characteristics, frequency dependency, non-linear stiffness and non-linear damping characteristics of bushings. However, their methods rely on the availability of component specific test data and further parametrization is required using external data fitting tools. To overcome these challenges, in another study, Lee and Kim, (2002) proposed a transfer function model method to treat Voigt model deficiencies that introduces polynomial fraction transfer function model to predict the slightly increasing complex stiffness characteristics over frequency. However, that study does not address the modelling of both material friction and complex damping characteristics of the bushings. The quick and easy determination of the stiffness and damping characteristics of

rubber bushings such as from vehicle level tests would be more advantageous instead of performing repeated component level testing for each bushing.

Along these lines, the objective of the paper is to propose a new methodology for the determination of the stiffness and damping characteristics of the rubber bushings from vehicle level tests and compare the new methodology with Voigt modelling method. This paper is organized as follows: Section 2 gives a short summary on characteristics of rubber bushings and their modeling methodologies such as Voigt models in the literature. Stiffness and damping characterization with simplified transfer function is explained in Section 3. Next, the proposed methodology is demonstrated on a heavy commercial truck on various durability roads along with comparison of the performance of the new method with that of Voigt model in Section 4. Finally, concluding remarks are made in the last section.

2. QUASI-STATIC AND DYNAMIC CHARACTERISTICS OF RUBBER BUSHINGS

Rubber bushings as vibration isolation components are extensively used in vehicle suspensions and engine mounting systems as vibration isolation components. In this section, the characteristics of rubber bushings and deficiencies of existing modelling techniques are discussed.

The measurement of vibration isolators involves quasi-static force-deflection measurements and dynamic sweep excitations at different amplitude of vibrations in order to characterize their complex energy dissipation, frequency and amplitude dependent characteristics.

Representative energy dissipation characteristics of a rubber bushing used in the cabin suspension of a heavy commercial truck obtained from quasi-static measurements is shown in Figure 1.a. As evident from the plot, the force-displacement characteristics is highly nonlinear. The results of dynamic sweep tests of vibration isolators showing the stiffness and phase angle of vibration isolators with frequency are shown in Figure 1.b and Figure 1.c, respectively. Among them, the phase angle is known to be related to the damping of a system and therefore it is shown to play a role in the energy dissipation of the system (Scheiblegger et. al., 2014). Regarding their frequency dependent behavior, it is also observed that while the stiffness of the component generally is reduced with increasing amplitude of excitation, the phase angle exhibits an increasing trend.

Figure 1.d shows the damping of a rubber bushing with respect to frequency from dynamic sweep tests. As evident from these graphs, the damping changes significantly over the frequency range from 0 to 20 Hz.

This is indicative of a high level of damping existing as part of the equivalent damping of the system, which has the potential of changing the response of the dynamic system significantly. This is especially true for the simulation of ground vehicles for vehicle dynamics and durability assessment since the frequency of the excitations due to the road surface covers frequencies up to 20 Hz. Therefore, viscous damping effect of the rubber bushings should be accounted for in simulation models in order to predict the durability loads at the engine mounts, suspension attachment points as well as to evaluate the vehicle ride and impact harshness metrics accurately.
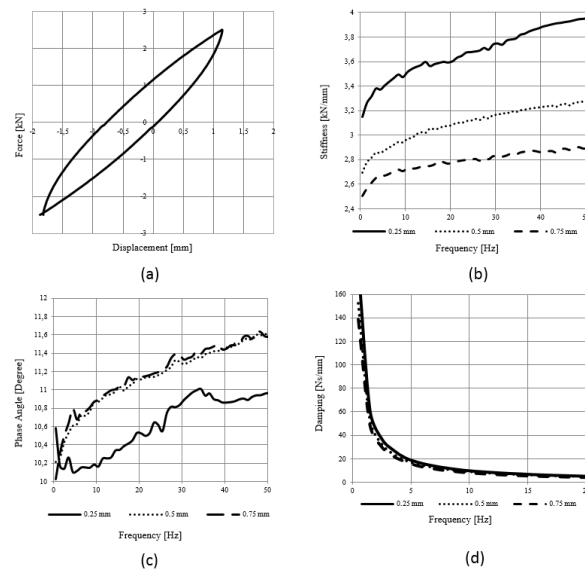

Figure 1: Quasi-static and dynamic characteristics of rubber bushings a. Quasi-static measurement, b. Stiffness versus frequency from dynamic sweep test, c. Phase angle versus frequency from dynamic sweep tests, d. Damping versus frequency from dynamic sweep tests

The Voigt model is widely used to represent the vibration isolator elements in multi body dynamics models and can be simply considered as a linear spring and damper element connected in parallel. The stiffness coefficient of the Voigt model can be obtained from the mean value of the real part of the complex stiffness over the frequency range of interest. The damping characteristic of the Voigt model is derived by measuring energy dissipation per cycle around the resonant frequency.

The use of Voigt models is limited to Single Degree-of-Freedom (SDOF) systems since they are only capable of predicting the system dynamics at a single frequency (Lee and Kim, 2002). Therefore, the Voigt models are not accurate alternatives for the representation of Multi-Degree-of-Freedom (MDOF) systems where there are multiple numbers of resonance

frequencies as in the case of automotive ride models (Scheiblegger, et. al., 2014).

3. Modelling of multi-DOF systems with simplified transfer function models

Traditional models of mechanical systems such as ground vehicles are based on lumped masses representing system parts and connection between parts being represented using proper constraint equations and elastic joints (Tebbe et. al.,2006). This modelling strategy, known as full-body modelling, is a very powerful technique for calculating many simulation outputs within models that correlate well to correlate well to real life conditions. Although extensively used in product development cycle with success, this modelling strategy has some drawbacks. One major disadvantage is that the creation of a full model depends on extensive number of parameters some of which may be difficult and/or costly to obtain. It may also be more difficult, at least for an inexperienced user, to relate the design parameters to the product performance. Another drawback of using complex system models is that it is more likely for them to demand longer simulation times and to experience numerical instabilities. Lengthy simulations become even more a bottleneck during design optimization studies where the model is calculated repetitive times. Therefore, existence of an effective analytical modelling approach that can accurately capture the dynamics of a system is vital. For example, cabin suspension system of a heavy duty truck is shown in Figure 2.a. Modelling the kinematics of the system's suspension, and obtaining the mass, inertia, center of mass of rigid bodies in the system model as well as the viscoelastic characteristics of its isolation elements and converting them to multi-body dynamics model is a challenging and time-consuming task. In Figure 2.b, corresponding MSC.ADAMS model of the full cabin suspension system following this modeling strategy is shown.

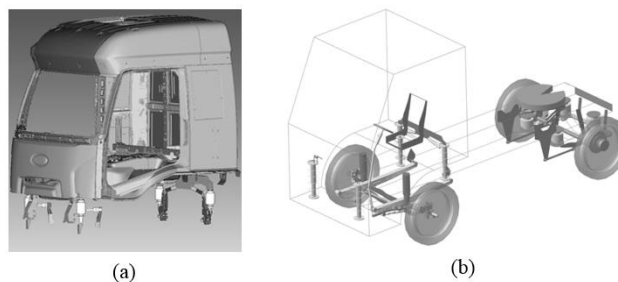(a)   (b)

Figure 2: (a) Cabin suspension system of a heavy duty truck (b) Multibody dynamics model of truck in MSC.ADAMS software

To address these aforementioned challenges, this paper proposes to follow a systematic approach based on a simplified mathematical model compared to calculate the durability loads at the cabin attachment points more accurately than the full model. The steps of the proposed approach are summarized as follows. The first step is to transform the full model of a truck to a simple model in order to simplify the modelling assumptions and eliminate the need for obtaining many input parameters (Section 3.1). Once the system model is simplified, the next step is to calculate the inertial force and moment at the center of gravity of the system during the durability tests (Section 3.2). Then, the equivalent stiffness of the viscoelastic elements (rubber bushings) is determined from the rigid body modes of the system (Section 3.3). Afterwards, damping characterization of the viscoelastic elements with simplified transfer function approach is performed before calculating the overall response of the simple model to road inputs (Section 3.4-Section 3.6).

3.1. Simplified System Model
The simplified model of the truck cabin suspension system, shown in Figure 3, only consists of the equivalent mass and inertia of the cabin at the center of gravity of the cabin and is connected to four bushings representing the overall stiffness and damping characteristics at the cabin attachment points.
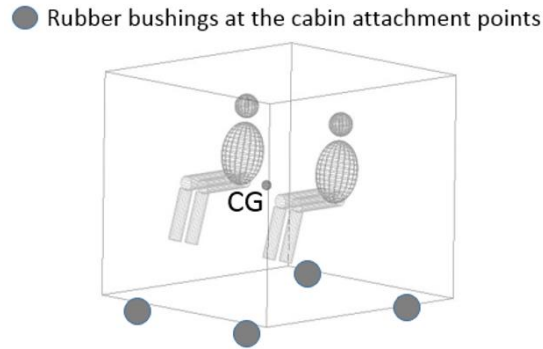

Figure 3: Simplified representation of the cabin model

Simplified model requires the determination of following information: 1) road excitation as input to the analytical model, 2) mass / inertia and center of gravity of the body, 3) equivalent stiffness properties of the rubber bushings and 4) damping characteristics of the rubber bushings as model parameters. The free-body diagram of the simplified system model is shown in Figure 4 and the equations of motion (EOM) are presented in vector form as in Equation (1) and Equation (2).
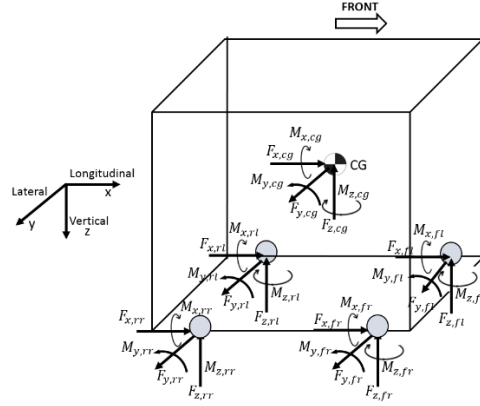
Figure 4: Free-body diagram of simplified system model

$$\vec{F}_{CG} - \left(\vec{F}_{fl} + \vec{F}_{fr}\right) - \left(\vec{F}_{rl} + \vec{F}_{rr}\right) = 0 \qquad (1)$$

$$\vec{M}_{CG} - \left(\vec{M}_{fl} + \vec{M}_{fr}\right) - \left(\vec{M}_{rl} + \vec{M}_{rr}\right) = 0 \qquad (2)$$

where subscripts fl, fr, rl and rr represent the front left, front right, rear left and rear right cabin attachment points, while subscript CG represents the center of gravity of the cabin. The subscripts x, y, and z represent the components of forces and moment in three directions, where F and M denote forces and moments, respectively.

3.2. Determination of Inertial Loads
Calculation of the inertial loads at the center of gravity (CG) of the cabin requires the determination of the acceleration vector of the CG of the cabin. Cabin CG accelerations are usually obtained by measuring at least six-channels for accelerations located at three locations of the cabin (referred to as A_{mes}). The equations used to calculate the acceleration of the cabin CG are shown in Equation (3) and Equation (4), where A_{CG} is an 6xN (N: number of measured data point) matrix containing translational and rotational accelerations of the cabin CG. Sensor locations should be selected such that the matrix B is non-singular (Yang et. al., 2014).

The inertial loads acting at the CG of the cabin are calculated by multiplying the acceleration matrix with the mass matrix given in Equation (5). The F_{CG}, matrix of size 6xN matrix, contains the translational forces and rotational moments in all directions acting at the CG of the cabin (Yang et. al., 2014).

$$B = \begin{bmatrix} 1 & 0 & 0 & 0 & z_2 & -y_2 \\ 0 & 1 & 0 & -z_2 & 0 & x_2 \\ 0 & 0 & 1 & y_2 & -x_2 & 0 \\ 0 & 0 & 1 & y_3 & -x_3 & 0 \\ 0 & 0 & 1 & y_1 & -x_1 & 0 \\ 0 & 1 & 0 & -z_3 & 0 & x_3 \end{bmatrix} \qquad (3)$$

$$A_{CG} = B^{-1} \cdot A_{mes} \qquad (4)$$

$$F_{CG} = m \cdot A_{CG} \qquad (5)$$

3.3. Determination of Equivalent Stiffness

Accuracy of the equivalent stiffness of rubber bushings is one of the key factors in establishing a simulation model that is well-correlated with the physical system of interest. The equivalent stiffness is derived from the calculated rigid body modes of the truck. Since the simplified model shown in Figure 4 has six DOFs (three translational and three rotational of the center of gravity of the cabin), it has six rigid body modes. The rigid body modes of the cabin and equivalent stiffness of the rubber bushings are related to each other as shown in Equation (6) to Equation (11). In these equations f_{fx}, f_{fy}, f_{fz} are translational rigid body modes in Hz, f_{tx}, f_{ty}, f_{tz} refer to rotational rigid body modes in Hz, where k_x, k_y, k_z represent equivalent stiffness of the system in N/m, m is mass of the body in kg and ρ_x, ρ_y, ρ_z are radius of gyration in meter in given directions, a_y and a_z are the longitudinal and vertical distance between the CG and the rear attachment points, respectively (Harris and Piersol, 2002).

$$f_{fx} = \frac{1}{2\pi} \sqrt{\frac{\sum k_x}{m}} \qquad (6)$$

$$f_{fy} = \frac{1}{2\pi} \sqrt{\frac{\sum k_y}{m}} \qquad (7)$$

$$f_{fz} = \frac{1}{2\pi} \sqrt{\frac{\sum k_z}{m}} \qquad (8)$$

$$f_{tx} = \frac{1}{2\pi} \sqrt{\frac{\sum (k_y a_z{}^2 + k_z a_y{}^2)}{m \rho_x{}^2}} \qquad (9)$$

$$f_{ty} = \frac{1}{2\pi} \sqrt{\frac{\sum (k_x a_z{}^2 + k_z a_x{}^2)}{m \rho_y{}^2}} \qquad (10)$$

$$f_{tz} = \frac{1}{2\pi} \sqrt{\frac{\sum (k_x a_y{}^2 + k_y a_x{}^2)}{m \rho_z{}^2}} \qquad (11)$$

3.4. Damping Characterization with Simplified Transfer Function Model

In the proposed method, the equivalent damping of the system is derived from the frequency response of the vehicle test measurement data that will be referred to as the target signal. The order and parameters of the transfer function are derived from the measurement of accelerations at various locations on the cabin (A_{mes} in Equation 4) and the accelerations are calculated from the simplified model.

A generic transfer function between the target signal (from vehicle measurement) and the simulation output is shown in Figure 5. It is a measure of discrepancy between the target signal and simplified model, and used to determine the damping characteristics as a function of frequency that needs to be incorporated to the simplified model. For instance, if the damping characteristic is of band damping type as shown in Figure 5.b, the damping of the viscoelastic element is modelled as in the given frequency bands shown in the figure. Similarly, for the transfer functions where damping characteristic is of increasing or decreasing behavior with frequency, the damping should be modelled as in Figure 5.c. Accordingly, the transfer functions for low damping, band damping and high damping types are formulated via Equation (12) to Equation (14), respectively.
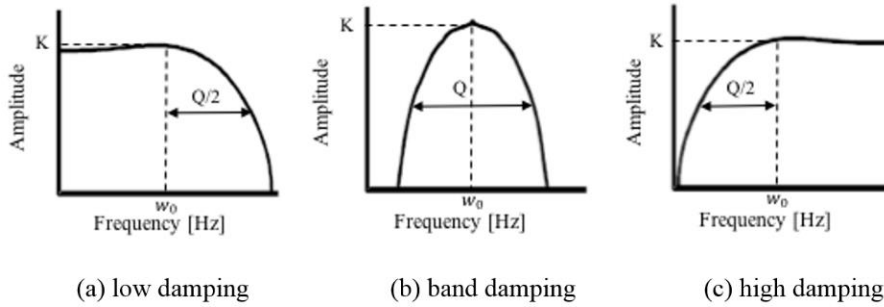

(a) low damping   (b) band damping   (c) high damping

Figure 5: Frequency dependent damping

$$TF_{low} = K \cdot \frac{\omega_0{}^2}{s^2 + \frac{\omega_0}{Q}s + \omega_0^2} \tag{12}$$

$$TF_{band} = K \cdot \frac{\frac{\omega_0}{Q} \cdot s}{s^2 + \frac{\omega_0}{Q}s + \omega_0^2} \tag{13}$$

$$TF_{high} = K \cdot \frac{s^2}{s^2 + \frac{\omega_0}{Q}s + \omega_0^2} \tag{14}$$

where $s = \sigma + j \cdot \omega$, where σ is amplitude or gain and ω_0 is the angular frequency. Q is the "quality factor", which is a unitless parameter for determining the bandwidth of the systems in frequency domain where higher Q indicates lower rate of energy loss corresponding to low damping

rate in the system. Therefore, the parameter Q determines system behavior in terms of its damping characteristics such as an overdamped, underdamped or critically damped system. In Equations (12) to (14), ω_0 determines the center frequency of the transfer function, where the damping value is the maximum. The parameters, Q and ω_0, determine the frequency range where there is effective damping in the system. Finally, the K term in the damping transfer functions in Equations (12) to (14), is the gain of the transfer function and scales the amplitude of the damping transfer function. Determination of the parameters of the transfer function is explained in the next section.

3.5. Determination of the transfer function parameters

The parameters of the simplified transfer function, K, Q and ω_0, are found by solving a nonlinear curve fitting problem. For this purpose, MATLAB's "lsqcurvefit" function is used to solve the general curve fitting problems by determining the coefficients of the parameters of the curve fit. It solves the curve fitting problem in least-squares sense, given by Equation 15, in order to find the coefficients of the function which is fit.

$$min\|F(x, x_{data}) - y_{data}\|_2^2 = min \sum (F(x, x_{data}) - y_{data})^2 \qquad (15)$$

given input data x_{data}, and the observed output y_{data}, where x_{data}, and y_{data} are matrices or vectors, and $F(x, x_{data})$ is a matrix-valued or vector-valued function of the same size as y_{data}. For the damping transfer function case, x_{data}, is the frequency data and y_{data} is the amplitude of the transfer function shown in Figure 6. For example, the function $F(\omega)$ corresponding to the amplitude of the band type damping transfer function is given in Equation (16).

$$F(\omega) = K \cdot \frac{\omega_0/Q}{\sqrt{(\omega_0^2 - \omega^2)^2 + (\omega_0/Q)^2}} \qquad (16)$$

The implementation code of the algorithm in MATLAB is presented in Figure 6.

```
clear;  close all;
% LOAD THE FREQUENCY VERSUS AMPLITUDE OF THE TRANSFER FUNCTION
transfer_function_data_new;
% THE DATA HAS A NX2 MATRIX (tfd) FIRST COLUMN FOR FREQUENCY IN HZ,
% SECOND COLUMN THE AMPLITUDE OF THE TRANSFER FUNCTION
w=tfd(:,1);     % Frequency in Hz
amp=tfd(:,2); % Frequency in m/s2
w_rad=w*2*pi; % Frequency in rad/s
xdata=w_rad;
ydata=amp;
% x(1):K ; x(2):w0 and x(3): Q
% Amplitude of the Transfer Function for Band-Damping
fun = @(x,xdata)(x(1)*x(2)/x(3))./(sqrt((x(2)^2-w_rad.^2).^2+...
    (x(2)/x(3).*w_rad).^2));
x0 = [100,12,0.35]; % Initial Conditions for w0, K and Q, respectively
% Calculation of the coefficients of the fit
x = lsqcurvefit(fun,x0,xdata,ydata);

K=x(1); % Parameter w0 of the band type damping transfer function
w0=x(2);  % Parameter K of the band type damping transfer function
Q=x(3);  % Parameter Q of the band type damping transfer function
```

Figure 6: Code for application of "lsqcurvefit" to find the parameters , K, Q and ω_0 in MATLAB

3.6. Metrics to Quantify the Accuracy of the Simplified Transfer Function Methodology

Two objective metrics to measure the accuracy of the simulation with respect to test data are chosen: 1) Coefficient of Determination 2) Root Mean Squared Error (RMSE). The coefficient of determination is a measure of how similar the shape of the simulation result is with respect to the test data. The coefficient of determination, shown by symbol r, is given by Equation (17). Its value can range from -1 to 1, i.e. $-1 \leq r \leq 1$, where r=1 is attained in case of the simulation results being perfectly correlated to test results.

$$r = \frac{n \cdot \Sigma(f \cdot y) - (\Sigma f) \cdot (\Sigma y)}{\sqrt{n \cdot (\Sigma f^2) - (\Sigma f)^2} \cdot \sqrt{n \cdot (\Sigma y^2) - (\Sigma y)^2}} \tag{17}$$

where y is the target signal (measurement data), f is the simulation signal of simplified model and n is the number of simulation data points.

Root Mean Squared Error (RMSE) is calculated according to Equation (18) as:

$$RMSE = \sqrt{\frac{1}{N} \Sigma_{i=1}^{n} (y_i - f_i)^2} \tag{18}$$

Similarly, y is the target signal (measurement data), f is the simulation signal and i represents the number of simulation data points in Equation 18.

Since the damping characterization of the transfer function is made by using the simple model and measurement data, it is expected that the shape of the frequency response of the simple model is forced to become similar to the test data resulting in higher coefficient of determination than Voigt model. Similarly, the RMSE between the simple model and test data is minimized when compared to the use of the Voigt model.

4. EXPERIMENTAL RESULTS

In this section, the proposed methodology will be demonstrated on a heavy commercial truck cabin for calculating the loads at the attachment points. Calculated values of the acceleration of the cabin attachment points are compared with vehicle measurements as well as the results from Voigt models in order to demonstrate the effectiveness of the proposed methodology.

A heavy commercial truck with a mechanical suspension system at both chassis and cabin is selected as an example to demonstrate the methodology. The selected truck is a 6x4 construction truck with 12.7 liter 6-cylinder engine with power of 420 PS at 1800 rpm and maximum torque of 2150 Nm operating with an engine speed of 1000-1300 rpm. The truck has a wheelbase of 3800 mm and tires of size 315/80 R22.5. The properties for mass, inertia properties, spring and damping rates of chassis and cabin suspension system are given in Table 1.

Table 1: The properties of the 6x4 truck

Parameters	Values
Chassis (front-rear) / Cabin Suspension (front-rear) Stiffness (N/mm)	37-370 / 50-40
Chassis (front-rear) / Cabin Suspension (front-rear) Damping (Ns/mm)	30-30 / 10-10
Truck Mass / Cabin Mass (kg)	24000 / 1200
Cabin Inertia $I_{xx,yy,zz}$ (kgm^2)	$7.3x10^8, 5.4x10^8, 8.1x10^8$

Vehicle parameters such as springs and dampers are either measured in-house or are obtained from the suppliers. The truck cabin mass and inertia are measured at Ford's Vehicle Inertia Measurement facility (VIMF). The VIMF test fixture measures the vehicle corner weights, center of gravity height, and the truck cabin inertias. The cabin was measured on the VIMF with a weight representing the driver on the cabin intended to represent the vehicle condition during the full-vehicle dynamic testing. This data was then used to ensure that the ADAMS model had weight, CG height, and

inertial properties that matched the prototype test vehicle. Kinematic and Compliance testing (K&C) is meant to be the first step in correlation of the subsystem's performance, thereby allowing the full-vehicle dynamic correlation of the CAE model to be close to test data in the early stages of the design process. The kinematic and compliant characteristics of the front and rear suspension systems were measured on the K&C test fixture. Then, this test data was compared to the results of an ADAMS full vehicle simulation run under the same conditions to assess the status of model correlation and verify the accuracy of the model's kinematic and compliant characteristics. There are several tests in K&C, in which vehicle performance parameters are investigated and correlated. These tests can be listed as bounce test, roll test, steering ratio test, lateral force compliance test (parallel & opposed directions) and aligning torque compliance test (parallel & opposed directions). Some of the correlation channels include suspension rate, wheel rate, steer angle, toe angle, camber angle, caster angle, lateral and longitudinal displacement of wheel center and steering ratio. Once the correlation results reach a satisfactory level in K&C testing, durability tests are conducted.

The chosen construction truck example has been tested on four different roads that are shown in Figure 7, namely road with humps, road with interspersed Belgian pave, cross country road and road with potholes and bumps. The objective of these tracks is to test the truck according to its customer correlated usage specifically in terms of simulating the combined vertical, longitudinal and lateral load conditions. Vehicle speed, which is measured by a speedometer, ranges from 10 kph to 30 kph on all roads.

Displacement and acceleration sensors have been instrumented on truck cabin and chassis frame for correlation purposes. Sensitivity of the accelerometers is 80 mV/g and they can measure between 1-2000 Hz up to a maximum acceleration of 50g. Specifications and mounting locations for the accelerometers are given in Table 2. Acceleration data from the accelerometers on the four cabin attachment points were synchronously measured at a sample frequency of 500 Hz using LMS Scadas. Due to high variance on the road conditions especially for off-road conditions, measurements have been repeated five times and the average of the measurements is used in the analysis. Acceleration data were first filtered using a Butterworth filtering function, where noise below 1 Hz and secondary vibration sources above 50 Hz such as engine were filtered out. The acceleration data were then processed using a block size of 1048 with a Hanning window and an overlap of 67%. The vehicle was tested in

unladen condition with the driver only in the truck cabin as part of the testing procedure.
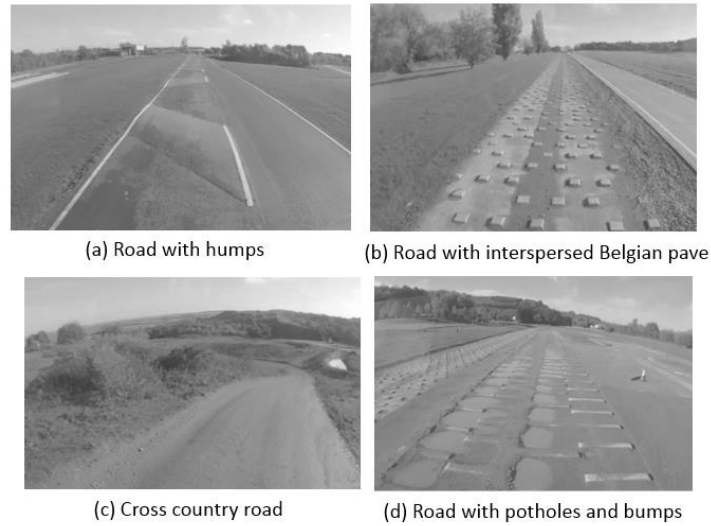

(a) Road with humps (b) Road with interspersed Belgian pave

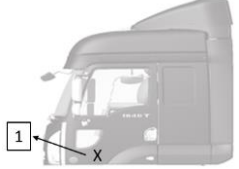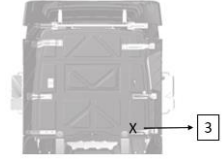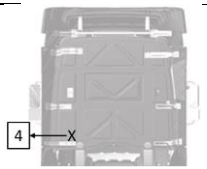(c) Cross country road (d) Road with potholes and bumps

Figure 7: Parts of the durability track

Table 2: Sensor locations and specifications

Sensor Location	Sensor Specification	Graphics
Front left	Silicon Designs DC type tri-axial accelerometer	
Front right	Silicon Designs DC type tri-axial accelerometer	
Rear left	Silicon Designs DC type tri-axial accelerometer	
Rear right	Silicon Designs DC type tri-axial accelerometer	

In the first step of the methodology, the inertial loads of the simplified model are calculated at the center of the gravity of the truck cabin using the acceleration measurements as described in Table 2 along with Equation (1) to Equation (3). The resulting vertical component of the inertial load is shown in Figure 8.
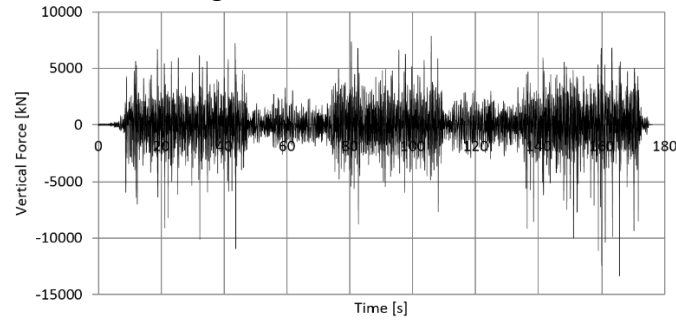

Figure 8: Vertical component of the inertial load at the CG of the cabin

The stiffness of the cabin bushings in each direction is manually tuned in order to match the six rigid body modes of the simplified model with the test results from four poster testing (Sendur et. al., 2016). These rigid body modes of the cabin obtained from four poster test is presented in Table 3. Equations (6) to Equation (11) are used to calculate stiffness of the system in each direction. The corresponding parameters obtained for the bushing rates (front-left, front-right, rear-left and rear-right attachment points) as a result of the tuning process to correlate to the four poster tests are presented in Table 4.

Table 3: Rigid body modes: simplified model versus four poster test

Description of the Mode	Simplified Model [Hz]	Four Poster Test [Hz]
Fore-Aft Mode	30.6	31.5
Lateral Mode	34.7	33.7
Bounce Mode	2.2	2.6
Roll Mode	1.7	2.4
Pitch Mode	1.2	1.5
Yaw Mode	18.7	13.6

Table 4: Translational and rotational stiffness of the attachment points

	Translational Stiffness [N/mm]			Rotational Stiffness [N/mm]		
	Kx	Ky	Kz	Ktx	Kty	Ktz
Front Left	7976	4600	52.1	572.9	4018.1	11.4
Front Right	7976	4600	52.1	572.9	4018.1	11.4
Rear Left	7976	4600	41.7	572.9	4018.1	11.4
Rear Right	7976	4600	41.7	572.9	4018.1	11.4

Frequency response of the simplified model is compared to the measurements from vehicle tests referred as target signal in Figure 9. The frequency spectrum in the figure refers to the vertical acceleration of the cabin front left attachment for the simplified model on the road with humps. The results show that there is a similarity on the peak frequencies between test and simulation results. For example, the peaks at 1-4 Hz band, 5-8 Hz band and 10-15 Hz bands in Figure 9 are well captured by the simplified model with equivalent stiffness of the bushings with respect to test signals that are characterized with rigid body modes given in Table 3. It can be concluded that the frequency based responses agree well with a relative error at frequencies which exhibit major amplitude peaks is less than %5 between the target signal and amplitudes calculated by the simplified model. Since the Voigt model is a linear spring with a linear viscous damper in parallel, its capability to correlate to real life scenario is limited. The stiffness and damping of the Voigt model can be tuned to match only one single frequency and the amplitude at corresponding frequency value. If a Voigt modeling approach were used, the model could be accurate on only one of the peaks in Figure 9.
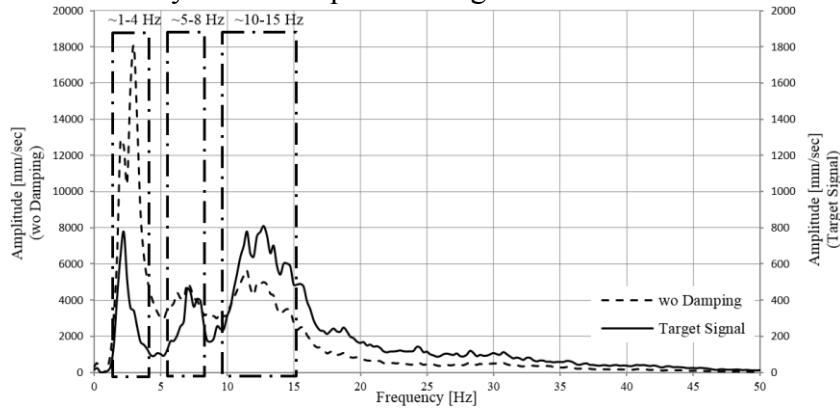

Figure 9: Comparison of frequency response of simple model (with equivalent stiffness and no damping) versus road test data

Once an acceptable correlation is achieved at frequencies with major amplitude peaks, we proceeded with calculation of the damping characterization of the rubber bushings. The damping transfer function is calculated by dividing the amplitude of the target signal by the amplitude calculated from the simple model. The resulting damping transfer function is given in Figure 10. The characteristics of the damping transfer function exhibits a similar behavior to the damping characteristics of the band-damping transfer function given by Equation (13) and is shown in Figure 5.b.
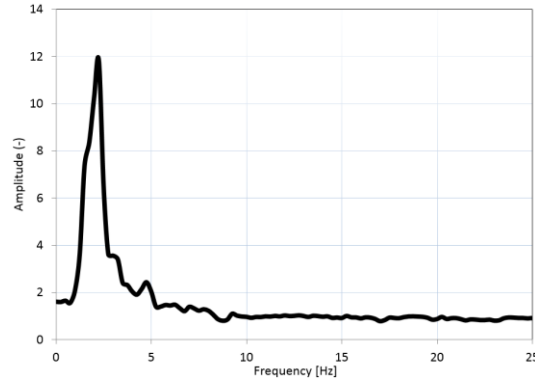
Figure 10: Amplitude of damping transfer function

The parameters of the damping transfer function are calculated using MATLAB's lsqcurvefit function as described in Section 3.5. The parameters of the simple transfer function correspond to the three outputs of the MATLAB function and are summarized in Table 5.

Table 5: Parameters of the band damping transfer function

Parameter	Value
ω_0 [Hz]	2.0
Q [-]	4.0
K [-]	167

The proposed methodology for damping characterization was implemented in the multi body dynamics modeling environment (MSC.ADAMS) with co-simulation via MATLAB/Simulink software as shown in Figure 11. Instantaneous velocities at the 4 cabin attachment points ($\dot{z}_{fl}$, $\dot{z}_{fr}$, $\dot{z}_{rl}$, $\dot{z}_{rr}$ are the vertical velocities of front-left, front-right, rear-left and rear-right attachment points, respectively) are calculated in MSC.ADAMS for every time step and are passed to MATLAB/Simulink as inputs to the damping transfer function calculations. Then, the damping forces at the cabin attachment points ($TF_{fl}(\dot{z}_{fl})$, $TF_{fr}(\dot{z}_{fr})$, $TF_{rl}(\dot{z}_{rl})$, $TF_{rr}(\dot{z}_{rr})$) are the vertical damping forces at the front-left, front-right, rear-left and rear-right attachment points, respectively) are calculated according to Equation (13) for the band-damping transfer function and output to MSC.ADAMS for the solution of the equation of motion. A similar numerical procedure is performed for the calculation of the spring forces. The vertical displacements corresponding to front-left, front-right, rear-left and rear-right ($z_{fl}, z_{fr}, z_{rl} \text{ and } z_{rr}$) are calculated in MSC.ADAMS and input to MATLAB/Simulink where the spring forces are calculated using the displacement information.
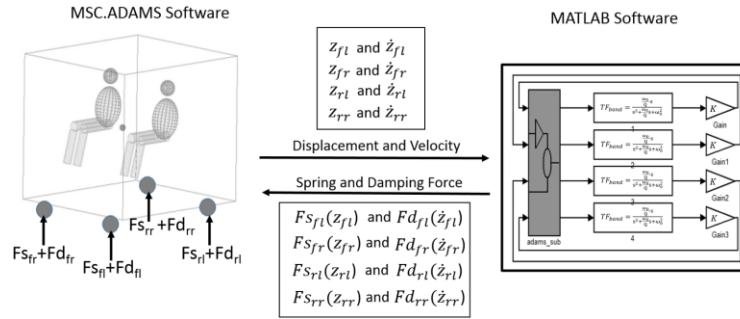
Figure 11: Methodology in multi-body simulation environment

The results for the vertical acceleration of front-left cabin attachment calculated by Simple Transfer Function (STF) and Voigt model are plotted on four road profiles given in Figure 7 and are presented in Figure 12 to Figure 15, respectively. Visual comparison of both methods with test data show that the STF has better correlation than Voigt model in terms of predicting the peaks and the amplitudes at corresponding frequency values. The coefficient of determination (%) and RMSE metrics between simple transfer function model and target signal are summarized in Table 6 along with the same metrics calculated for Voigt model and target signal in order to compare both methodologies, objectively. Higher coefficient of determination values is representative of closer similarity in the predicted shape curves of the methodology versus the target signal. Similarly, lower RMSE values are an indication of reduced errors between the simulation method and target signal. Accordingly, the results show that STF has higher coefficient of determination to target signal than Voigt model on all the road profiles which were considered in this study. The performance of the STF method is also better than Voigt model based on the RMSE metric for all the road profiles. The objective metrics are aligned with the visual comparison of the two methods.
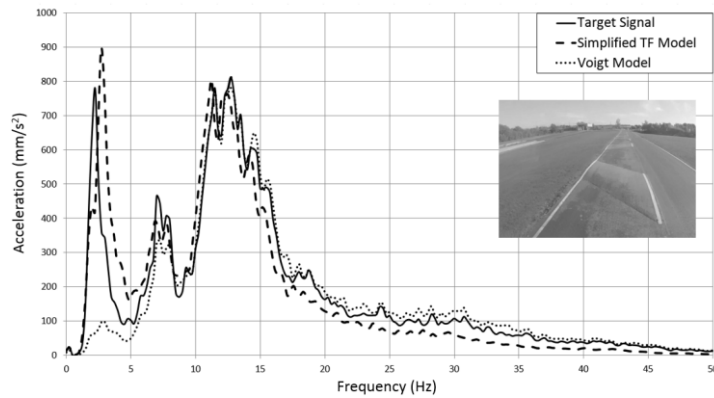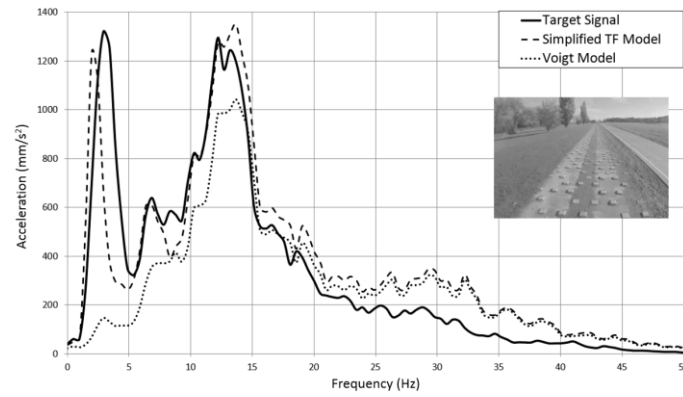

Figure 12: Results on road with humps

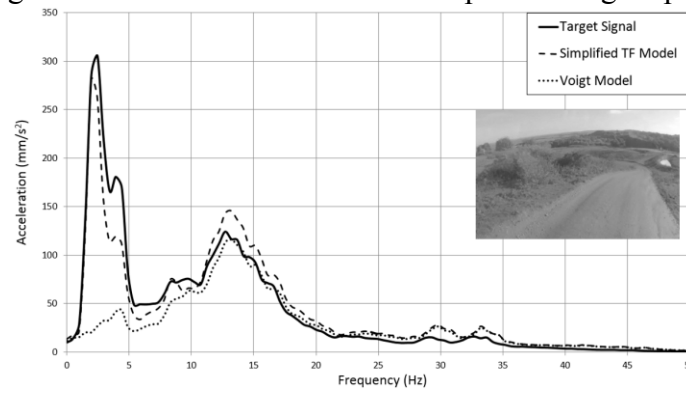Figure 13: Results on road with interspersed Belgian pave

Figure 14: Results on cross country road

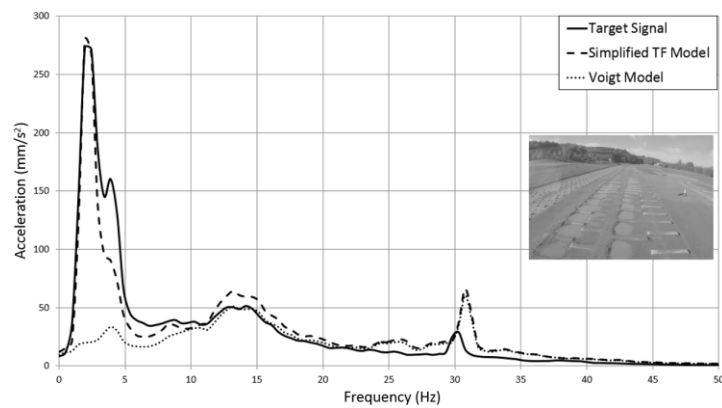Figure 15: Results on road with twist humps

Table 6: Comparison of STF model and Voigt model

	Coefficient of Determination (%)		RMSE (mm/s2)	
	STF model	Voigt model	STF model	Voigt model
Road with twist humps	93	83	1068	1227
Road with interspersed Belgian pave	89	86	1721	3285
Cross country road	98	70	157	512
Road with potholes and bumps	96	86	150	468

5. CONCLUSIONS

Effective use of simulation models during the design cycle depend on many factors among which the quality of the simulation model stands out. The model quality is an indication of both the complexity of the simulation model and its accuracy. While the number of input parameters and the computational time directly depend on the complexity of a simulation model, the accuracy of the simulation model determines its validity for the design cycle. In this paper, a simple modeling approach to predict the loads in multi-body systems and the determination of the viscoelastic properties of the model are proposed. This approach enables the simulations with minimum number of inputs. Furthermore, the limitations of widely used Voigt model in representing the viscoelastic characteristics of rubber bushings are pointed out in this study and a new methodology to overcome the limitations of the Voigt model is proposed. More specifically, the limitations of the current modelling of rubber bushings with respect to its damping representation were explained, and a new modelling approach is devised. The proposed model addresses the damping characterization of the rubber bushings by a band pass filter based general transfer function form covering upper and lower bounds, where the parameters can be easily tuned using the nonlinear curve fitting function in MATLAB. The implementation of the proposed methodology in the multi body dynamic simulation environment is explained with full body co-simulations in MSC.ADAMS via MATLAB/Simulink software.

The validity and effectiveness of the methodology is demonstrated in the calculation of durability loads at the cabin attachment points of a heavy duty truck experienced on various durability roads. A simple 6 DOF cabin model is proposed with the equivalent compliance and kinematic properties as the full vehicle model in order to calculate the durability loads at the cabin attachment points. The system is modeled by a lumped mass approach where the cabin is represented by mass, inertia and center of gravity and the cabin kinematics is represented by overall equivalent

bushings. This representation eliminates the modelling of all system while requiring a less number of input parameters. As illustrated in the case study, the representation of the damping in rubber bushing is of significant importance for accurate model behavior. The damping is characterized by a simple transfer function where the parameters are determined by the application of a formal curve fitting problem. The accuracy of the methodology with respect to the test data was compared based on two metrics: the coefficient of determination and root mean-squared error (RMSE). The relation between the parameters characterizing the damping transfer function in order to improve the accuracy of the simulation model with respect to physical testing are also presented. As the results show, the agreement of the simplified transfer function methodology with test data and the improvement of the accuracy of the methodology compared to the Voigt model prove the potential of the proposed methodology for modeling the viscoelastic properties of rubber bushings.

6. REFERENCES

[1] Li, S., Yang, X., Minaker, B., and Lan, X. (2015), *"Development of a Nonlinear, Hysteretic and Frequency Dependent Bushing Model",* SAE Technical Paper 2015-01-0428, DOI:10.4271/2015-01-0428.

[2] Scheiblegger, C., Roy, N., Silva, O.P., Hillis, A., Pfeffer, P. and Darling, J. (2014), *"Non-linear Modeling of Bushings and Cab Mounts for Calculation of Durability Loads"*, SAE Technical Paper, DOI: 10.4271/2014-01-0880.

[3] Lee, J. H. and Kim, K. J. (2002), *"Treatment of Frequency-Dependent Complex Stiffness for Commercial Multi-Body Dynamic Analysis Programs"*, Mechanics of Structures and Machines, Vol. 30, No. 4, pp. 527-541, DOI: 10.1081/SME-120015075

[4] Sedlaczek, K., Dronka, S., and Rau, J. (2011), *"Advanced Modular Modelling of Rubber Bushings for Vehicle Simulations"*, Vehicle System Dynamics, 49 (5) :741-759.

[5] Zhang, L., Liu, H., Zhang, H., and Xu, Y. (2011), *"Component Load Predication from Wheel Force Transducer Measurements"*, SAE Technical Paper 2011-01-0737, 2011, DOI: 10.4271/2011-01-0737.

[6] Cao, C., Ghosh, S., Rao, R. and Medepalli, S. (2005), *"Truck Body Mount Load Prediction from Wheel Force Transducer Measurements"*, SAE Technical Paper 2005-01-1404, DOI: 10.4271/2005-01-1404.

[7] Gauerhof, L., Bilic, A., Knies, C., and Diermeyer, F. (2016), *"Integration of a Dynamic Model in a Driving Simulator to Meet Requirements of Various Levels of Automatization",* IEEE Intelligent Vehicles Symposium (IV), Gothenburg, Sweeden.

[8] Yang, X., Muthukrishnan, G., Seo, Y., and Medepalli, S. (2004), *"Powertrain Mount Loads Prediction and Sensitivity Analyses"*, SAE Technical Paper 2004-01-1691, DOI: 10.4271/2004-01-1691.

[9] Scheiblegger, C., Roy, N., Silva. P., and Hillis, A. (2014), *"Non-Linear Modeling of Bushings and Cab Mounts for Calculation of Durability Loads"*, SAE Technical Paper: 2014-01-0880, DOI:10.4271/2014-01-0880.

[10] Spencer, B., Jr., Dyke, S., Sain, M., and Carlson, J. (1997), *"Phenomenological Model for Magnetorheological Dampers"*, Journal of Engineering Mechanics, 10.1061/0733-9399, Volume: 123(3), pp. 230-238.

[11] Ok, J., Yoo, W. and Sohn, J., (2008), *"New Nonlinear Bushing Model for General Excitations using Bouc-Wen Hysteretic Model"*, International Journal of Automotive Technology, Volume: 9(2), pp. 183–190.

[12] Tuncel, O., Sendur, P., Ozkan, M., Guney, A. (2010), *"Ride Comfort Optimization of Ford Cargo Truck Cabin"*, International Journal of Vehicle Design, Vol. 52, Issue 1-4, Issue 1-4, DOI: 10.1504/IIJVD.2010.029645

[13] Papalambros, P. Y., and Wilde, D. (2000), *"Principles of Optimal Design: Modeling and Computation (2nd edition)"*, Prentice Hall, ISBN: 978-0521627276

[14] Sendur, P., Kurtdere, A., and Akaylar, O. 2016, *"Methodology to Improve Steering Wheel Vibration of a Heavy Commercial Truck"*, Internoise 2016, Hamburg

[15] Tebbe, J. C., Chidambaram, V., Kline, J.T., Scime, S., Shah, M. P. Tasci, M., Zheng, D. (2006), *"Chassis Loads Prediction using Measurements as Input to an Unconstraint Multi-Body Dynamic Model"*, SAE Technical Paper, DOI: 10.4271/2006-01-0992

[16] Sendur, P. (2002) *"Physical System Modeling: Algorithms for Assessing Model Quality Based on Design Specifications"*, Ph.D. Thesis, The University of Michigan, Ann Arbor, MI

[17] Harris, C. M. and Piersol, A. G. (2002), *"Shock and Vibration Handbook"*, McGraw Hill, 5th Edition, DOI: /10.4271/2006-01-0992

[18] Aydemir, E. (2016). *"Prediction of a Frequency Dependent Heavy Commercial Vehicle Cabin Loads by Using Acceleration Signals,"* M.Sc. Thesis, Yildiz Technical University, Istanbul.

[19] Oppenheim, A.V., Schafer, R. W. (1975), *"Digital Signal Processing (1st Edition)"*, Pearson, 1st Edition, ISBN: 978-0132146357

[20] Srinath, M.D., Rajasekaran, P. K., Viswanathan, R. (1995), *"Introduction to Statistical Signal Processing with Applications"*, Prentice Hall, 1st Edition, ISBN: 978-0131252950